# Projected changes in both mean climate and climate variability drive substantial increases in extreme fire weather in the western United States

Danielle Touma[a,b] & Clara Deser[b]

[a] *Jackson School of Geosciences, Institute for Geophysics, University of Texas at Austin, Austin, TX*

[b] *Climate and Global Dynamics, National Center for Atmospheric Research, Boulder, CO, USA.*

*Corresponding author*: Danielle Touma, danielle.touma@utexas.edu

ABSTRACT

Wildfire frequency, extent and duration in the western United States (U.S.) is projected to increase throughout the 21st century as dry and warm conditions become more frequent, widespread, and persistent. However, it is still unknown how changes in mean climate and changes in climate variability, individually and together, contribute to these increases. To disentangle these effects, we use a 100-member ensemble of climate simulations produced with the Community Earth System Model v2 under historic and SSP3-7.0 forcing from 1980-2100. Using the Canadian Forest Fire Weather Index (FWI) to quantify fire-related meteorological conditions in the simulations, we select extreme FWI thresholds relative to a baseline distribution centered at 1980 ("fixed threshold") and an evolving distribution ("moving threshold") to identify spatiotemporally connected extreme fire weather events. By 2100, the frequency, area, and duration of events increase when considering a fixed threshold, and events are up to 4°C warmer on average. Moreover, events over the Pacific Coast expand northwestwards, while those over the Four Corners region expand westwards and northeastwards. Changes in event characteristics are small and not significant when considering a moving baseline but become spatiotemporally more connected. Increases in the mean of maximum temperature, as well as changes in both the variability and mean of relative humidity, drive the largest increases in extreme fire weather event area and duration. By quantifying how changes in the mean and variability of climate variables impact wildfire conditions in the western U.S., our study has implications for increasing resiliency to wildfire risk under climate change.


## 1. Introduction

Wildfire area and severity has increased in much of the Pacific Coast and Four Corners regions of the United States (U.S.) over the last few decades (Jones et al. 2022). Additionally, wildfires in recent years have become more synchronous, occurring in different parts of the North American continent simultaneously, and compounding the impacts felt in the region (Abatzoglou et al. 2021). For example, in 2023, unprecedented wildfires in both the western U.S. and Canada were burning simultaneously, reducing the capacity for coordinated firefighting and leading to poor air quality in much of the U.S. and Canada (Jones et al. 2024; Kirchmeier-Young et al. 2024). The increases in the area and severity of wildfires have been attributed to anthropogenically-forced anomalous warming and drying in recent years (Jain et al. 2022; Juang et al. 2022), over a century of forest fire suppression (Andela et al. 2017;

Jones et al. 2022) and increases in human-caused ignition (Balch et al. 2017). The damages felt by society due to these increases have also risen, with larger populations and more resources being exposed to wildfire hazards (Burke et al. 2021). Moreover, these larger and more frequent wildfires have exacerbated populations' exposure to smoke and post-fire hydrologic hazards, such as debris flows and channel sedimentation (Oakley 2021). These impacts have both short term and long term impacts on hydrology (Collar et al. 2022; Williams et al. 2022), livelihoods (Lawrence et al. 2022), and public health (Burke et al. 2021) in the western U.S.

Many studies have assessed trends in fire weather conditions - dry, warm and windy conditions – using fire weather indices such as the Canadian Forest Fire Weather Index (FWI) and the McArthur Forest Fire Danger index (FFDI), and their impact on the likelihood, frequency, and area of wildfires in recent years. Observed increases in extreme fire weather events lead to increases in burned forest area and higher wildfire frequency globally and in the western U.S. (Abatzoglou and Williams 2016; Goss et al. 2020; Jain et al. 2022; Jones et al. 2022). These increases largely stem from increases in maximum temperature and decreases in relative humidity prior to and during wildfire seasons, which have been linked to an increase in the frequency and intensity of atmospheric ridging in the northeast Pacific Ocean (Sharma et al. 2022). The Four Corners region has also been impacted by "failed" North American monsoon seasons as well as delays in monsoon onsets, leading to longer-than-usual dry conditions and subsequently higher wildfire activity (Cook and Seager 2013; Hoell et al. 2022). Changes in these conditions in the western U.S. are largely driven by increases in global greenhouse gas emissions and localized reductions in aerosol emissions (Abatzoglou and Williams 2016; Kirchmeier-Young et al. 2017; Touma et al. 2021). In future years, projected increases in greenhouse gas emissions and continued reductions in aerosol emissions are expected to lead to further increases in frequencies and durations of extreme fire weather conditions, leading to higher risks of wildfires, and causing the frequency of extreme fire weather conditions at the end of the 21$^{st}$ century to be well beyond the expected historic frequency, with fire weather conditions reaching a "new normal" (Abatzoglou et al. 2019; Touma et al. 2021, 2022).

Several studies have used singe-model and multi-model large ensemble Earth System Model (ESM) simulations to quantify the trends in fire weather conditions in future climate projections. There is a large consensus of increasing fire weather conditions over much of the globe when accounting for both model discrepancies (Abatzoglou et al. 2019; Bui et al. 2024) and irreducible internal variability (Kirchmeier-Young et al. 2017; Touma et al. 2021). Given systemic biases in ESMs, especially in the representation of the FWI (Gallo et al. 2023; Touma et al. 2021) and the driving variables (Fasullo, 2020; Simpson et al., 2024), the general approach is to use upper tails of a fire weather index distribution to define “extreme” fire weather within each ESM. Here, we compare the more traditional choice of using “fixed” historic or pre-industrial distributions of fire weather indices to calculate upper-tail thresholds to describe “extreme” fire weather conditions to the choice of using a moving-window threshold (hereafter, “moving threshold”), which captures the time-evolving distribution of fire weather conditions. While a moving threshold would ensure that the frequency of fire weather days for a specific location remain constant through time, the intensity and duration of events could still increase through changes in the variability beyond the extreme threshold. Moreover, spatial clustering or connectivity of extreme fire weather events could also increase, leading to greater spatially compounding risks, for example multiple wildfires occurring simultaneously, increased area and density of smoke from wildfire emissions, and preconditioning larger areas to post-fire hydrologic hazards (Raymond et al. 2020; Zscheischler et al. 2020). Using a moving threshold can also reveal additional criteria for adaptation measures needed to overcome changes in extreme climate events (Amaya et al. 2023).

Few studies have assessed how changes in the variability of the climate system, and not just the mean of the climate, has impacted wildfire risk under anthropogenic forcing. By doing so, changes in the variability are assumed to be negligible or part of the “noise” of our climate system – however, this could lead to the underestimation of the impact of anthropogenic forcing on wildfire risk. Zhuang et al. (2021) found that changes in atmospheric circulation, or natural variability, explained one-third of the observed vapor pressure deficit increase over the western U.S. in recent decades, but did not assess the roles of other atmospheric variables important for wildfire risk. While their study leveraged multi-model simulations from the CMIP6 archive, single-model initial-condition large ensembles could provide a more robust estimate of these influences by overcoming uncertainties from model physics (Deser et al. 2020; Zhuang et al. 2021).

In this study, we use the 100-member Community Earth System Model v2 Large Ensemble (CESM2-LE) to assess projected changes under SSP3-7.0 (Rodgers et al. 2021).

We show how extreme fire weather events respond to anthropogenic climate change in terms of their frequency, duration, spatial connectivity and extent, and intensity. We use both a fixed and moving-window period to calculate location-specific extreme percentile thresholds and identify spatiotemporally connected grid points as extreme fire weather events. We isolate the changes in climate drivers that impact the duration, area, frequency and intensity of these events. This study fills an important gap of understanding the role of changes in climate variability on wildfire risk and introduces a framework to isolate the impacts of changes in the mean from changes in the variability on extreme climate events using a large ensemble.

## 2. Data and Methods

### *a. CESM2-LE simulations*

We use the CESM2-LE simulations to quantify historic and future fire weather. As demonstrated in previous studies (e.g., Kirchmeier-Young et al., 2017; Touma et al., 2021, 2022), using a large ensemble allows robust assessment of changes in extreme fire weather events under anthropogenic forcing as well as internal variability. The CESM2-LE consists of 100 members and has daily resolution data publicly available, making it a unique and unprecedented dataset to understand future projections of extreme fire weather events.

The CESM2 model is a fully coupled atmosphere, ocean, land, and sea-ice model on a nominal 1-degree grid. The 100 members of the CESM2-LE are simulated under historic (1850-2014) and SSP3-7.0 (2015-2100) scenarios (Rodgers et al. 2021). The relatively high level of forcing in the SSP3-7.0 scenario enables the detection and quantification of forced changes in the mean and natural variability, making it suitable for our study. We note that all 100 members use identical forcing, except for the biomass burning aerosols. Half of the members follow the CMIP6 protocol for biomass burning, which consists of low-pass filtered (11-year smoothing) timeseries except over the period 1990-2020 when high-frequency satellite-based measurements are available. This introduces a discontinuity in temporal variance of biomass burning aerosols, which in turn has been shown to produce a rectified effect on climate conditions over high northern latitudes in association with Arctic sea ice feedbacks (e.g., DeRepentigny et al., 2022). For this reason, the other half of the members use 11-year smoothed biomass burning timeseries over the entirety of the simulations (see Rodgers et al. 2021 for additional information).  We find no discernable differences between the two halves of the CESM2-LE members for our analysis and therefore consider all 100 members together.

*b. Canadian Forest Fire Weather Index (FWI)*

We use a modified version of The Canadian Forest Fire Weather Index (FWI) to quantify fire weather conditions in the simulations. The FWI is widely used, both operationally and in understanding the impact of climate change on wildfire risk (Abatzoglou et al. 2019; Touma et al. 2021, 2022, 2023). The FWI was empirically derived by Wagner (1987) and its calculation is clearly described in Dowdy et al. (2009). The FWI is calculated for the CESM2-LE using surface daily precipitation (CESM2 variable name: PRECT, CMIP name: *pr*), maximum temperature (TREFHTMX, *tmax*), relative humidity (RHREFHT, *rhs*), and surface windspeed (WSPDSRFAV, *sfcWind*). We first quantify moisture conditions for three surface levels and time scales using three different moisture codes. The Fine Fuel Moisture Code (FFMC) reflects moisture levels for shaded litter fuels and on daily time scales and is calculated using *pr, tmax, rhs,* and *sfcWind*. The Duff Moisture Code (DMC) reflects moisture levels for decomposed organic material and on monthly timescales and is calculated using *pr, tmax*, and *rhs*. The Drought Code (DC) reflects moisture levels for deep litter and soil and is computed using *pr* and *tmax*. Using the FFMC and *sfcWind*, the Initial Spread Index (ISI) is then calculated to represent the fire spread rate, and using the DMC and DC, the Build-Up Index (BUI) is calculated to represent the potential heat release and severity of fire. Lastly, the ISI and BUI are used to calculate the FWI and represents overall fire danger. All moisture codes and indices are unitless.

*c. Extreme event definition and baselines*

To identify extreme fire weather events, we use the location-specific 99$^{th}$ percentile of the FWI across the full 100-member ensemble. Using the full ensemble to calculate the 99$^{th}$ percentile allows us to robustly account for internal climate variability when estimating extreme values. We use two baseline types to calculate the 99$^{th}$ percentile threshold and associated FWI variable (*pr*, *tmax*, *rhs*, and *sfcWind*) anomalies: (1) a "fixed" baseline 35-year period centered around 1980, and (2) a "moving" baseline 35-year period centered around each year in the timeseries. Therefore, the threshold using the fixed baseline is constant in time, while that with the moving baseline changes from year-to-year. Figure 1 shows an example of these thresholds and identified exceedances for a grid point near Los Angeles.

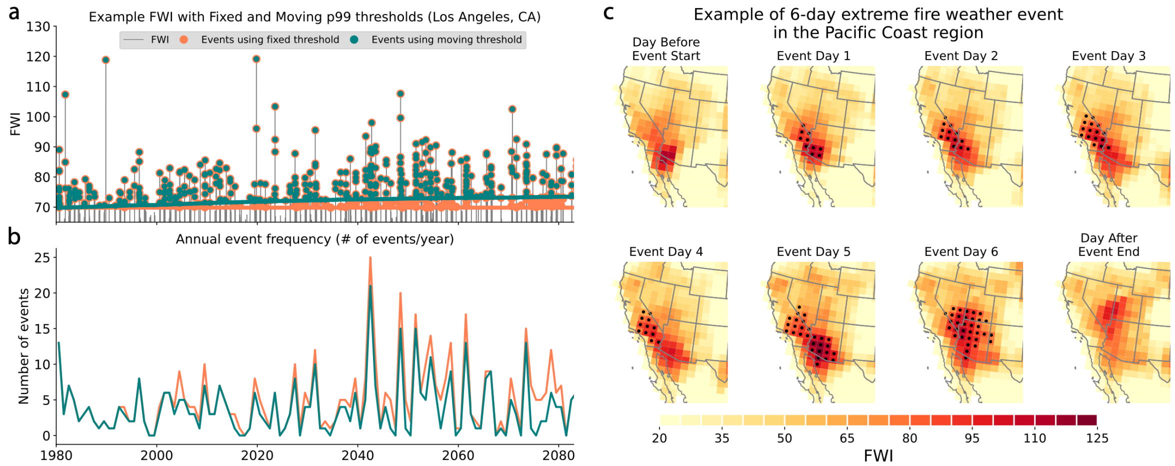


Fig. 1. a) Example FWI time series for one grid point near Los Angeles and one ensemble member (1001.001), with fixed and moving 99th percentile thresholds and identified exceedances (events). b) Annual number of events calculated from (a) for fixed and moving thresholds. c) Example of a 6-day extreme fire weather event over the Pacific Coast region. The shading represents the value of FWI, and the black dots represent the identifies spatiotemporally connected event. The event starts when at least one grid point in the regional boundary (see Figure 3) exceeds the local threshold and the event ends when there are no longer any grid points that are spatiotemporally connected to that event within the region boundary.

### *d. Event identification*

For each ensemble member and each threshold type, we identify grid points that have extreme FWI values for each timestep. We use a framework with image processing functions from the *Scipy* Python package (Virtanen et al. 2020) to identify spatiotemporally connected grid points that exceed the extreme threshold. We first spatially subset the FWI dataset from 0-90°N and 0-180°W to increase computational efficiency but ensure that events are not truncated spuriously. We then create a binary dataset, where grid points that meet or exceed the extreme threshold are equal to 1, and those that fall below the threshold are equal to 0. We then identify spatiotemporally connected grid points that are equal to 1 – for spatial connectivity, grid points must be connected by their edges or vertices and for temporal connectivity, at least one grid point within the event must be equal to 1 on two continuous days. The duration and cumulative area of each event is calculated, as well as the corresponding FWI values and variable anomalies throughout the event.

To understand the regional impact of changes in extreme fire weather events, we subset events for different regions (e.g., Southern California) and region groups (e.g., Pacific Coast).

To do so, we find events that have at least one grid point within the bounds of a region or region group of interest for the full duration of the event. If an event in the full event dataset “leaves” the region or region group and then “returns”, it is considered two distinct events. For region groups, we subset the dataset for the full region group simultaneously. This ensures that we do not double count events when events span multiple regions simultaneously. We show an example of a 6-day event over the Pacific Coast region in Figure 1c.

*e. Event analysis*

For each event, we calculate its total duration, total area, area within the region, mean FWI, maximum FWI, and mean anomalies of *pr, tmax, rhs*, and *sfcWind* using the fixed baseline and using the moving baseline. We create annual distributions of event characteristics for each season and region by first averaging over all events in each ensemble member in each season and region and then grouping those averages together to create a distribution (100 values representing an ensemble member each). We summarize these time-evolving distributions using the 25$^{th}$, 50$^{th}$, and 75$^{th}$ percentiles, or the interquartile range (IQR). We also count the number of events per year for each ensemble member in each season and region, and create similar annual distribution time series.

We also create composites for each period and each ensemble member for grid point- and event-specific values of the number of events, total number of event days, event duration, regional and total area, mean and maximum FWI, as well as *pr, tmax, rhs*, and *sfcWind* anomalies. All anomalies are calculated from grid-point specific 30-day moving window climatologies using either the fixed baseline period or 35-year moving window periods. We specify which type of baseline is being used when describing any relevant results.

*f. Regional and period definitions*

We identify eight U.S. regions and two region groups that have historically experienced large and severe wildfires. Washington (WA), Oregon (OR), northern and southern California (CA) are grouped in the Pacific Coast region, and Colorado (CO), New Mexico (NM), Arizona (AZ), and Utah (UT) are grouped in the Four Corners region.

We use three time periods to summarize extreme fire weather event characteristics over time. These are a historic period (1980-2014), an early future period (2015-2050), and a late future period (2051-2082). We end the last period in 2082 because we use 35-year moving windows to calculate the moving thresholds and means. We calculate changes in the characteristics of fire weather events for the two future periods relative to the historic period. Additionally, we show time series of extreme fire weather event characteristics for the eight regions, with changes computed from the historic period.

*g. Isolating the impact of changes in the mean and variability of FWI variables*

We isolate the effect of changes in *pr*, *tmax*, *rhs*, and *sfcWind* on the characteristics of extreme fire weather events. We create new "mapped" ($m$) time series for each variable and ensemble member ($n$) ($pr_m^n, tmax_m^n, rhs_m^n, and\ sfcWind_m^n$) using quantile mapping in order to restrict the whole time series to the 100-member monthly distribution in the fixed reference period using the following steps. For each day of the time series, we first find the percentile of the value of the variable within its 100-member, 30-day, 35-year moving window distribution. We then find the corresponding value of that percentile in the 30-day, 35-year, 100-member distribution of the fixed baseline period centered around 1980 (Figure 2). By mapping the FWI variable time series to the fixed period, we maintain the relative day-to-day variability and spatial patterns between the mapped variable and the other unmapped variables but ensure that the variability and mean of the timeseries is constrained to that of the historic distribution. We then calculate four "mapped" FWI time series for each ensemble member using one of the newly mapped variables and keeping the other variables at their original values ($o$) ($e.g., FWI_{pr,m}^n = f(pr_m^n, tmax_o^n, rhs_o^n\ , sfcWind_o^n)$). Using these four mapped FWI timeseries for each ensemble member, we identify and quantify the characteristics of extreme fire weather events as previously described. These events and their characteristics are considered to represent events in which one of the variables is not impacted by forced changes in the mean *and* variability. We then compare the event characteristics using the mapped and original FWI time series to assess the contribution of changes in the full distribution (i.e., mean and variability) of each variable to changes in extreme fire weather events.

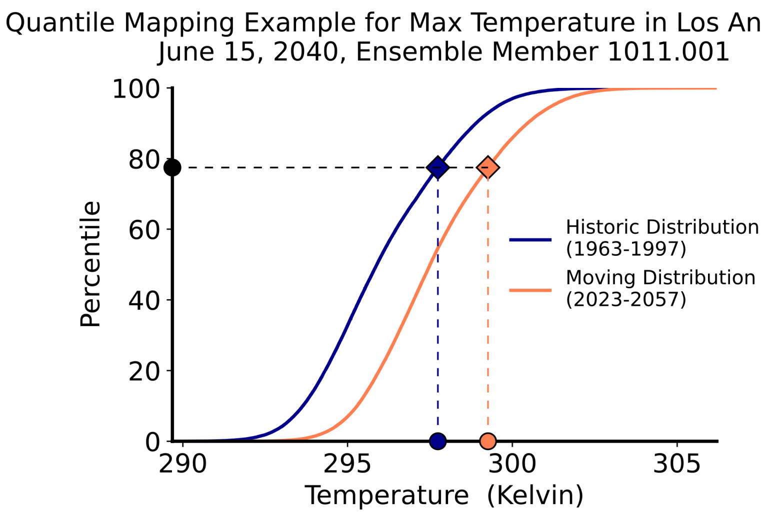


Fig. 2. Schematic of quantile mapping for maximum temperature for June 15, 2040 for a grid point near Los Angeles, CA for ensemble number 1011.001 using its 100-member moving distribution (June 1-30, 2023-2057) and the 100-member historic (June 1-30, 1963-1997) distribution. The coral (blue) line and markers represent the moving (historic) distribution and values, respectively.

We also create new time series with only forced changes in the mean removed for each variable. By comparing to the original time series, we isolate the impact of forced changes in the mean of each variable on extreme fire weather event characteristics. For each variable, we calculate forced changes in the mean using the difference between the moving 30-day, 35-year, 100-member mean and the fixed (1980) 30-day, 35-year, 100-member mean. We then remove these forced changes in the mean from each respective time series for each ensemble member to create four new "detrended" (*d*) time series $(pr_d^n, tmax_d^n, rhs_d^n, and\ sfcWind_d^n)$. As before, we use these new time series to calculate the FWI four additional times, each time using one of the new timeseries with the mean removed for one of the variables, while all other variables use their original time series $(e.g., FWI_{pr,d}^n = f(pr_d^n, tmax_o^n, rhs_o^n\ , sfcWind_o^n))$. Using these four new FWI timeseries for each ensemble member, we identify and quantify the characteristics of extreme fire weather events as previously described. These events and their characteristics are considered to represent events in which one of the variables is not impacted by forced changes in the mean. The difference between the quantile mapped and the detrended extreme fire weather events is used to estimate the effect of changes in the variability on the seasonal average of that variable.

## 3. Results

*a. Historic characteristics of extreme fire weather events*

Figure 3 shows composite maps of the number of extreme fire weather event days per year for the Pacific Coast and Four Corners regions using fixed and moving thresholds for June, July and August (JJA) – the height of the wildfire season in the western U.S. During the historic period, the fixed baseline shows similar patterns to the moving baseline though with smaller magnitudes because the time period used for the fixed threshold is slightly earlier than the moving threshold centers used in the composite maps (1963-1997 vs 1980-2014) (Figure 3 a, d, g, and j). We find that events that are partially or fully located in the Pacific Coast region tend to occur more frequently on the eastern side of the region (~1.5 events/year) relative to coastal areas (~0.75 events/year), and tend to extend further eastwards into Montana, Idaho, Nevada and Arizona (~1 event/year), southward into Baja California and northward into western Canada (Figure 3 a and g). Four Corners events largely occur in Arizona and Utah (~1.5 events/year), with fewer events occurring in Colorado and New Mexico, especially across the Rocky Mountains. Similarly, these events spread towards the north, reaching Idaho and Wyoming, and towards the west, reaching into Nevada and California (Figure 3 d and j). While the thresholds set the number of event days per year for each location in the historic period, these composite maps reveal that the geographic extent and duration of extreme fire weather events can differ for different regions.

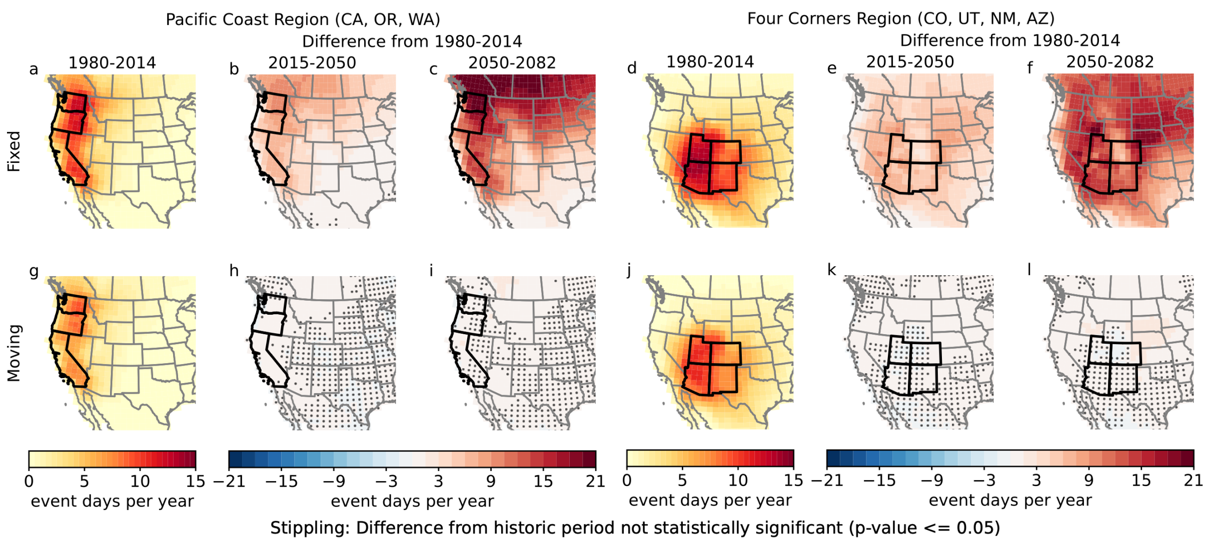


Fig. 3. Summer season (JJA) total number of event days per year over each grid point in the (a, d, g, and j) historic period (1980-2014) and change in number of events per year over each grid point in future periods (b, c, e, f, h, i, k, and l) using fixed (a-f) and moving (g-l) threshold for events fully or partially located in the Pacific Coast (a-c and g-f) and in the Four Corners (d-f, j-l) regions.

*b. Projected changes in extreme fire weather event characteristics*

Extreme fire weather events become more frequent, last longer, and cover larger areas by the end of the 21st century when using the fixed threshold compared to the moving threshold (Figures 3 and 4). In the Pacific Coast, events tend to become more frequent in the eastern parts of the region and more widespread towards the north and east, with up to an additional ~15 event days/year reaching the Midwest, and an additional ~21 event days/year reaching western Canada in the late future period (Figure 3 c). The largest increases occur in Washington, with approximately two more events/year, which also last two more days on average and cover 20,000 $km^2$ more in the late future compared to the historic period (Figure 4 d, h, and l). In the southern part of the region, increases in event duration and area are still significant but are slightly reduced in magnitude, with the smallest increases occurring in Southern CA (Figure 4 e and i). Events tend to become more connected and extend in all cardinal directions in the Four Corners region in the future compared to the historic period, with the largest spread towards southern Idaho and Nebraska (>15 more event days/year; Figure 3 e and f). Here, we find that extreme fire weather event duration and area increase similarly across all four states – events are approximately one day longer and cover approximately 5,000 $km^2$ more than in the historic period (Figure 4 q-x). Interestingly, increases in event area and extent are constrained by the Southern Rocky Mountain Range, but not by the Middle or Northern/Canadian Rocky Mountain Ranges for both the Pacific Coast and Four Corners regions (Figure 3).

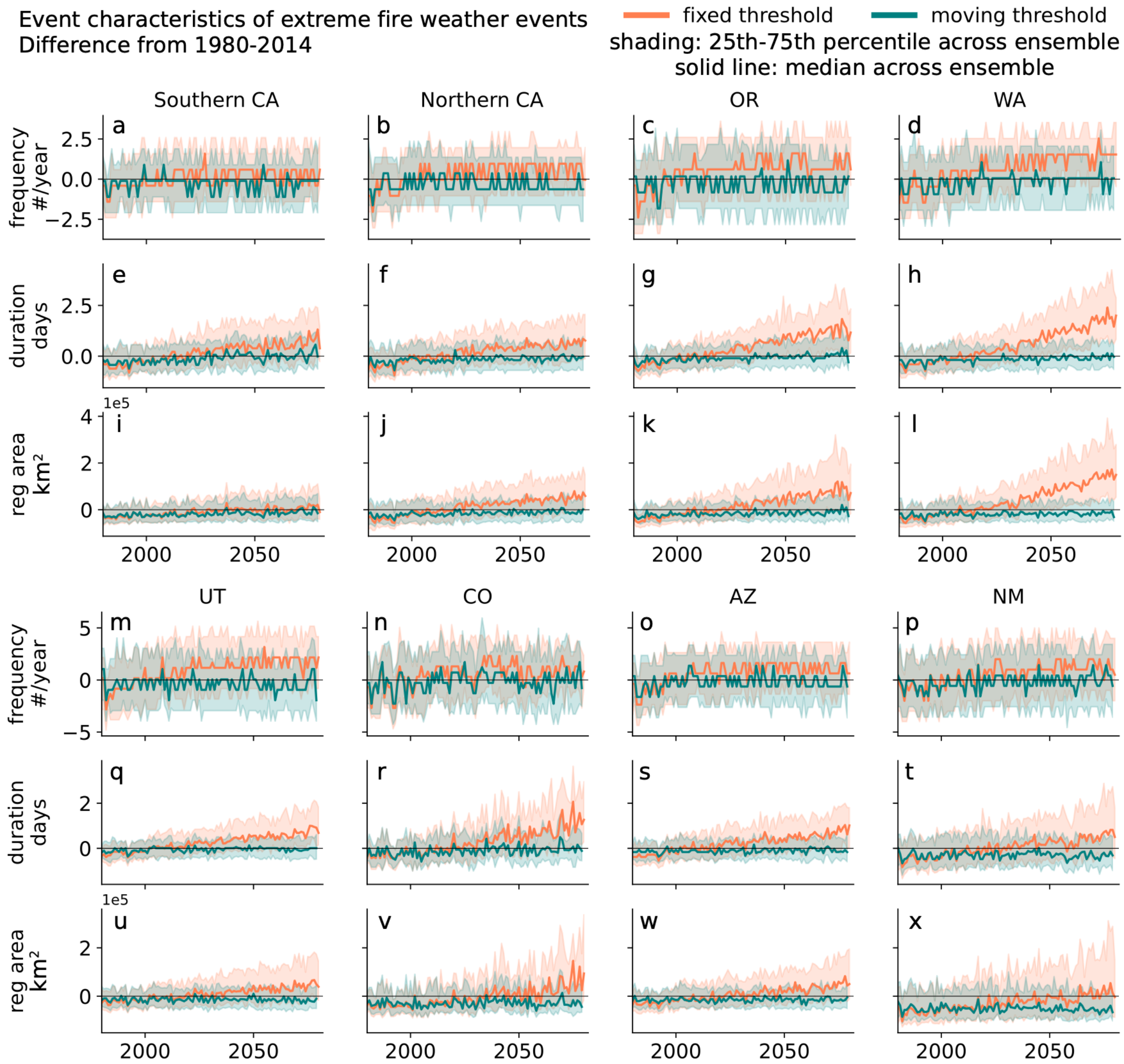


Fig. 4. Summer season (JJA) frequency (a-d and m-p), duration (e-h and q-t), and state-bound area (i-l and u-y) of extreme fire weather events using a fixed (coral) and moving (teal) 99th percentile threshold for events in the Pacific Coast (a-l) and Four Corners (m-y) regions.

While the annual frequency of events for each location using the moving threshold is explicitly set by the threshold (top 1% of events), the duration and spatial connectivity of the events is not explicitly bounded. Specifically, these 1% of events could occur more closely together in both space and time due to changes in the spatial or temporal variability of the FWI, and therefore could change the area and duration of events. We see some evidence of small but robust increases in the number of event days, generally occurring to the north and east of the Pacific Coast region and to the northeast and northwest of the Four Corners region (Figure 3 h and i). While this points to events becoming more widespread, changes in event duration are negligible using the moving threshold in the Pacific Coast and Four Corners region throughout both future periods (Figure 4). Therefore, moving-threshold exceedances are becoming more clustered in space on a given day but not necessarily becoming more clustered in time.

*c. Meteorological conditions underlying future changes in extreme fire weather events*

In the Pacific Coast region, extreme fire weather events in the historical period are characterized by positive anomalies in maximum temperature (up to 10 degrees K) and wind speed (up to 2 m/s), and negative anomalies in relative humidity (up to -25%) and precipitation (up to -2 mm/day) (Figure 5 a, d, g, j, n, p, s and v). In the late future period, extreme fire weather events identified using a fixed threshold show an increase in maximum temperature anomalies by up to 4 degrees Kelvin throughout the Pacific Coast region compared to the historic period (Figures 5 i and 6 e-h). Changes in other FWI variables are more spatially heterogeneous: precipitation anomalies tend to become less negative over California and more negative over Oregon and Washington; relative humidity anomalies tend to become less negative over the coast (+4%) and more negative over the interior of the region (-4%); and windspeeds tend to be about 0.5 m/s slower over the northern half of the region but unchanging in the southern part of the region (Figures 5 b, c, n, o, t, and u, and 6 a-d and i-p). When using a moving threshold and moving climatologies for the FWI variables, future increases in temperature anomalies during extreme fire weather events are more muted compared to using a fixed historic threshold, with warming generally < 1 K (Figures 5 k and l, and 6 e-h). However, precipitation anomalies become much more negative throughout the Pacific Coast region, decreasing by about 10% in some locations, with larger decreases occurring in the eastern part of the region (Figures 5 e and f, and 6 a-d). Despite events becoming drier, changes in the area, frequency, and duration of events are relatively small when using a moving threshold (Figures 3 h and I, and 4 a-l). Changes in relative humidity and wind speed are spatially varied and coincide with changes using the fixed threshold, but with smaller magnitudes – events on the coast become more humid, while interior events become less humid, and events in the north are less windy, while events in the south see increases in windspeed (Figures 5 w and x, and 6 i-p).

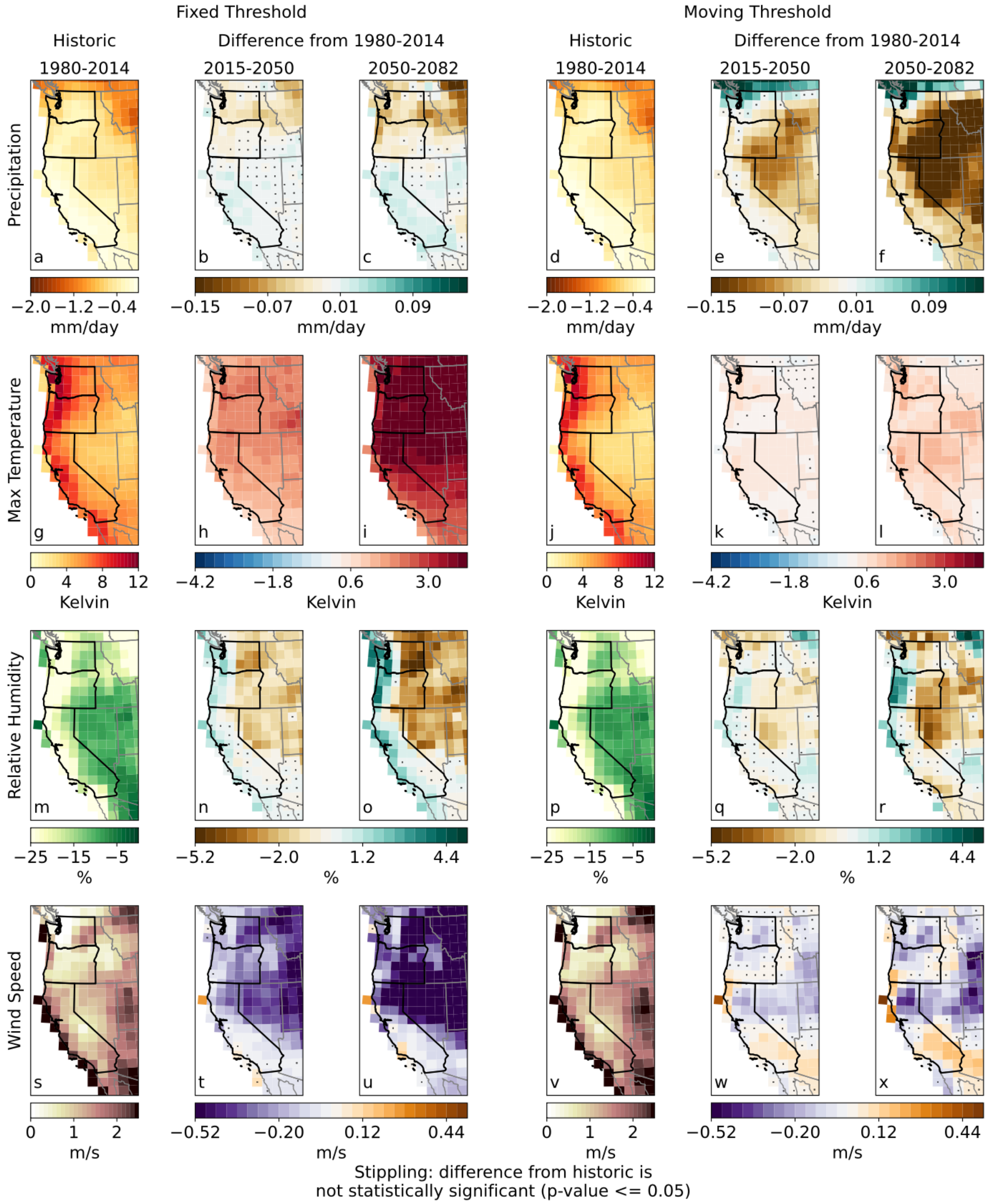


Fig. 5. Composite maps of FWI variables during extreme fire weather events using (a-c, g-i, m-o, s-u) fixed and (d-f, j-l, p-r, v-x) moving distributions for calculating the 99th percentile FWI threshold and FWI variable anomalies for the Pacific Coast region. The composites are created by averaging the variable anomalies over the area and duration of all events across all ensemble members in each period.

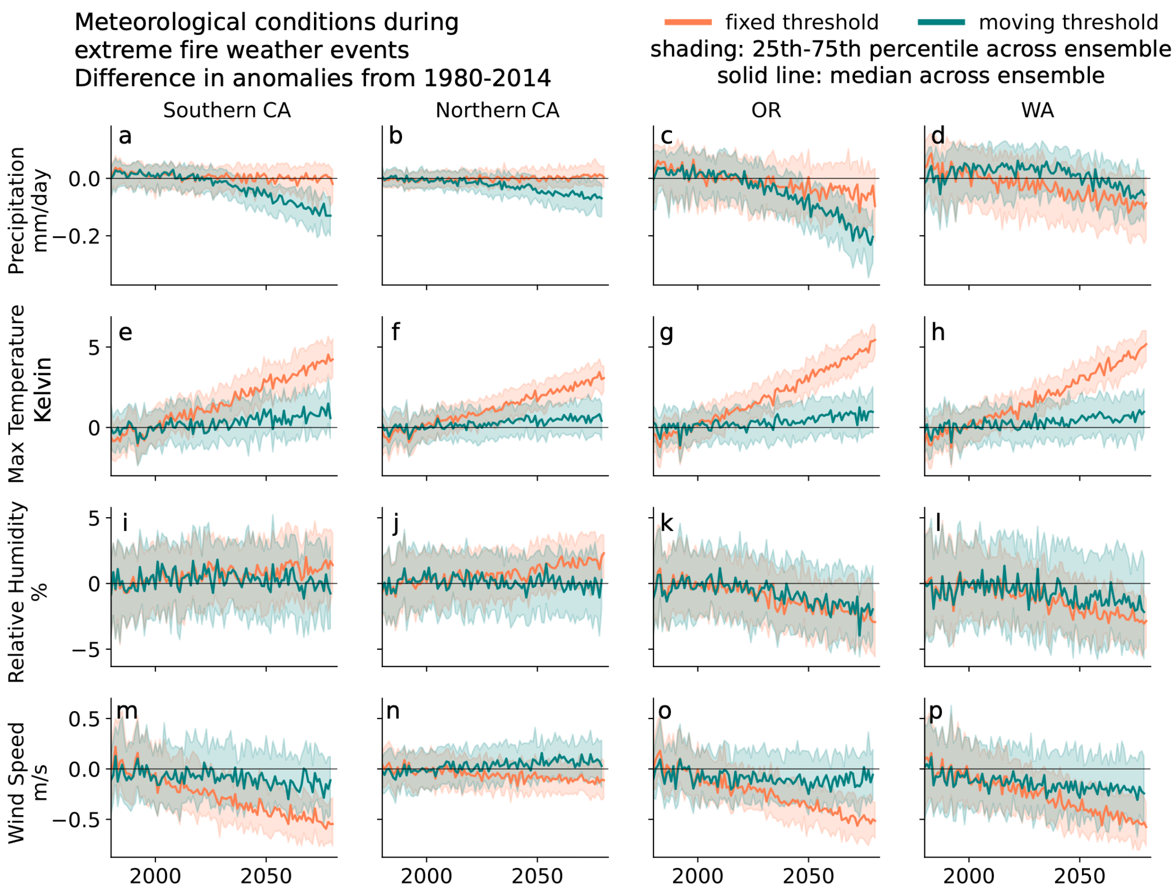


Fig. 6. Time series of precipitation (a-d), maximum temperature (e-h), relative humidity (i-l) and wind speed (m-p) during extreme fire weather events in JJA in Southern California (CA; a, e, i, m), Northern CA (b, f, j, n), Oregon (OR; c, g, k, o) and Washington (WA; d, h, l, p) using the fixed mean and threshold (coral) and the moving mean and threshold (teal).

Events identified using a fixed threshold in the Four Corners region also show large future increases in maximum temperature of up to 4 K (Figure 7 c). The largest increases in maximum temperature occur in Utah and Colorado, coinciding with decreases in relative humidity and increases in windspeed (Figures 7 c, e, g and 8 e, f, i, j, m, n). Events in the Rocky Mountains are relatively drier, with an average decrease of 0.15 mm/day in precipitation and 2% in relative humidity – however, this area shows relatively smaller increases in the number of event days/year (Figures 3 e and f, and 7 a and e). As in the Pacific Coast, events are generally less windy, with about 0.5 m/s decreases in windspeed over Utah and Colorado (Figures 7g and 8 m, n). Patterns similar to those in the Pacific Coast region emerge for events identified using a moving threshold in the Four Corners region. Events are much drier, especially in the center of the region, and Utah and western Colorado show large decreases in relative humidity (Figures 7f and 8 i, j). Events have greater windspeeds in New Mexico and Arizona, but lower windspeeds in the northern part of the Four Corners region

(Figures 7h and 8 m-p). Additionally, increases in maximum temperature are small and not significant for many parts of the region (Figures 7d and 8 a-d).

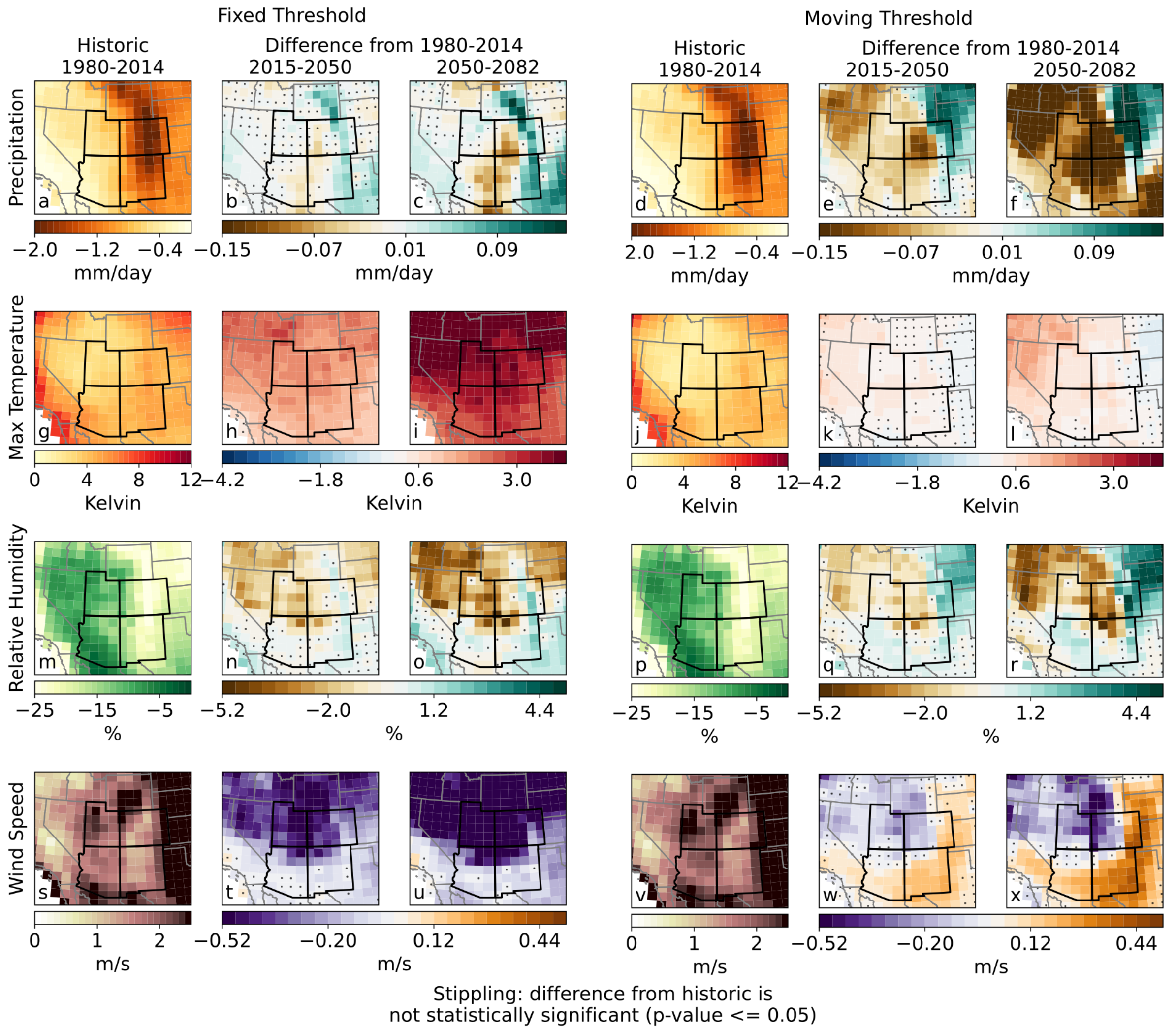


Fig. 7. Composite maps of FWI variables during extreme fire weather events using (a, c, e, g) fixed and (b, d, f, h) moving distributions for calculating the 99th percentile FWI threshold and FWI variable anomalies for the Four Corners region. The composites are created by averaging the variable anomalies over the area and duration of all events across all ensemble members in each period.

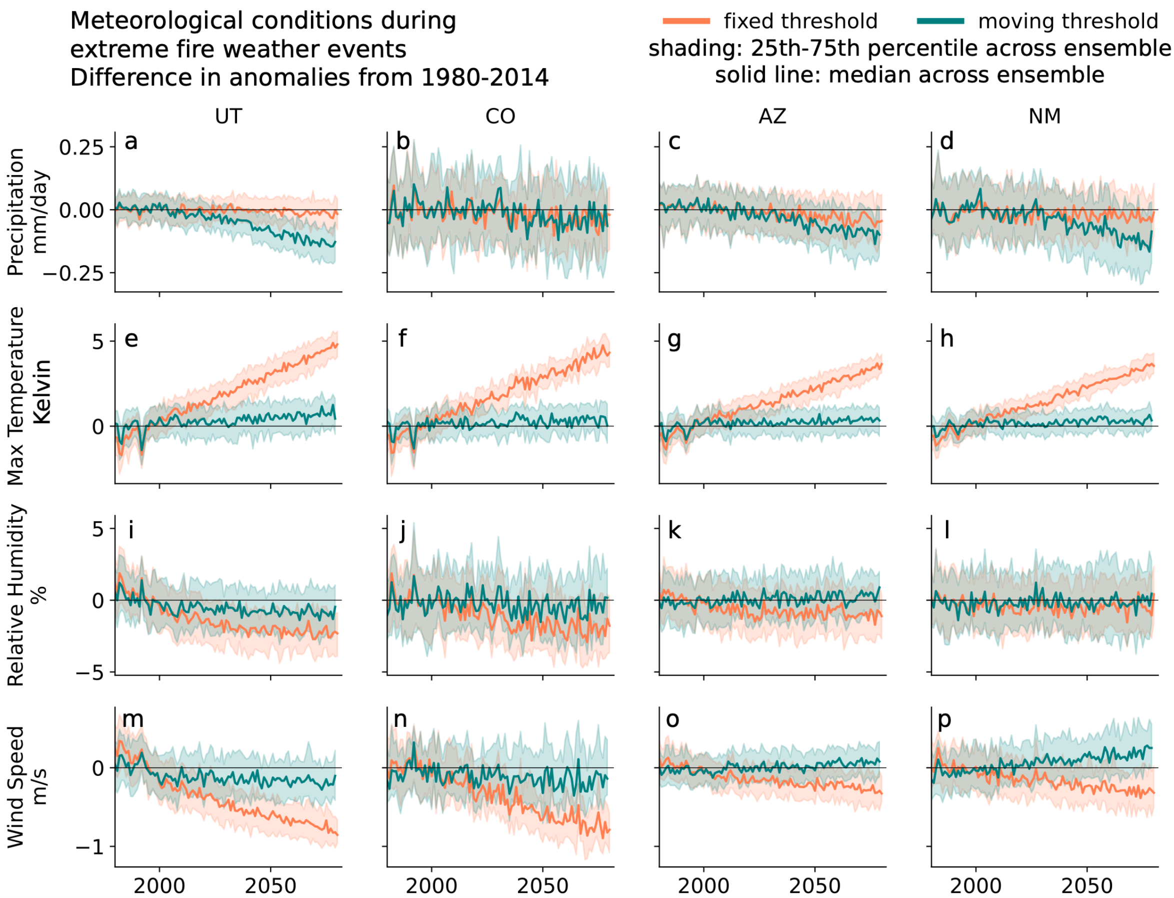


Fig. 8. Time series of precipitation (a-d), maximum temperature (e-h), relative humidity (i-l) and wind speed (m-p) during extreme fire weather events in JJA in Utah (UT; a, e, i, m), Colorado (CO; b, f, j, n), Arizona (AZ; c, g, k, o) and New Mexico (NM; d, h, l, p) using the fixed mean and threshold (coral) and the moving mean and threshold (teal).

### *d. Isolating the impact of individual fire weather variables*

While the previous results show how the underlying conditions of extreme fire weather events are projected to change, it is still unclear how changes in the mean and variability of each fire weather variable impact event characteristics. To investigate this, we use quantile and mean mapping approaches (see Methods) to isolate the impact of total changes, as well as changes in the mean and variability of maximum temperature, precipitation, relative humidity, and wind speed on the frequency, duration, area, and intensity of extreme fire weather events (identified using the fixed threshold) in the future periods for the Pacific Coast and Four Corners regions.

In the Pacific Coast region, mean increases in maximum temperature lead to the largest increases in extreme fire weather event frequency (up to ~1 event/year in some locations), duration (~10 event days), area (~10,000,000 km$^2$) and maximum FWI (~3 FWI units) in the late future period, while changes in the variability ("Difference") of maximum temperature have minimal impacts on these event characteristics (Figure 9 i, v, I and V compared to j, w, J, W). For all events in the Pacific Coast, mean changes in temperature also have the largest impact on event days per year, area, and intensity compared to changes in other variables (Figure 10 b-d). However, mean changes in temperature have relatively small or negligible impacts on event frequency, with the ensemble spread spanning zero (Figure 10 a).

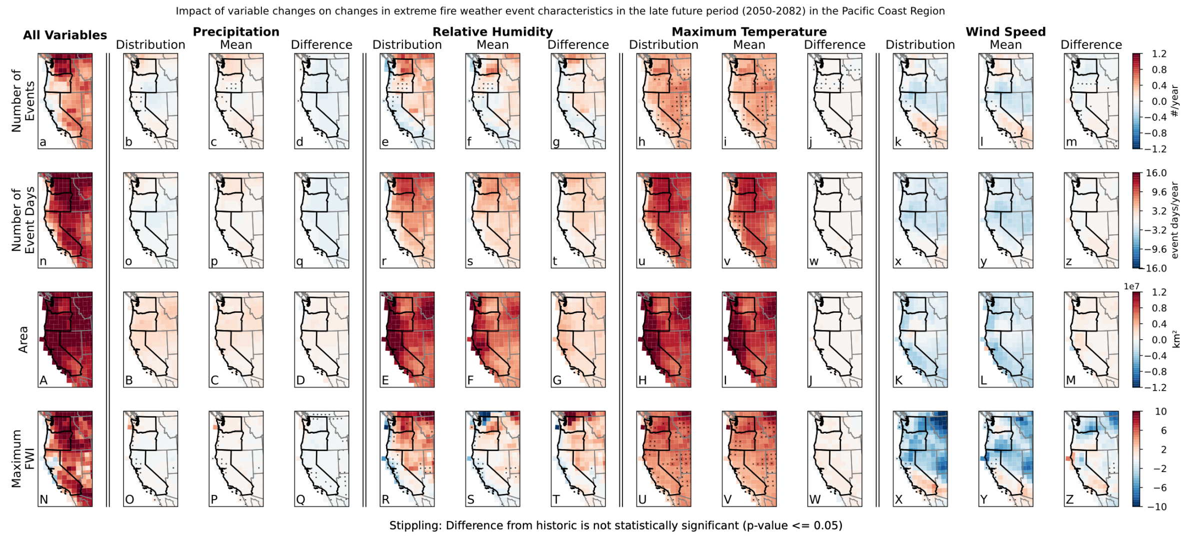


Fig. 9. The impact of changes in all variables (a, n, A, N), and the full distribution (b, e, h, k, o, r, u, x, B, E, H, K, O, R, U, X), means (c, f, i, l, p, s, v, y, C, F, I, L, P, S, V, Y) and variabilities ("difference"; d, g, j, m, q, t, w, z, D, G, J, M, Q, T, W, Z) of precipitation (b-d, o-q, B-D, O-Q), relative humidity (e-g, r-t, E-G, R-T), maximum temperature (h-j, u-w, H-J, U-W) and wind speed (k-m, x-z, K-M, X-Z) on changes (from the historic period, 1980-2014) in events per year (a-m), events days per year (n-z), event area (A-M), and maximum FWI (N-Z) using the fixed threshold in the late future period (2050-2082) for the Pacific Coast region. These composites are created by averaging event characteristics for all events for each ensemble member for each period at each grid point. Then, the grid point-specific values of the historic period are subtracted from each future period for each ensemble member, and the difference values are averaged over all ensemble members.

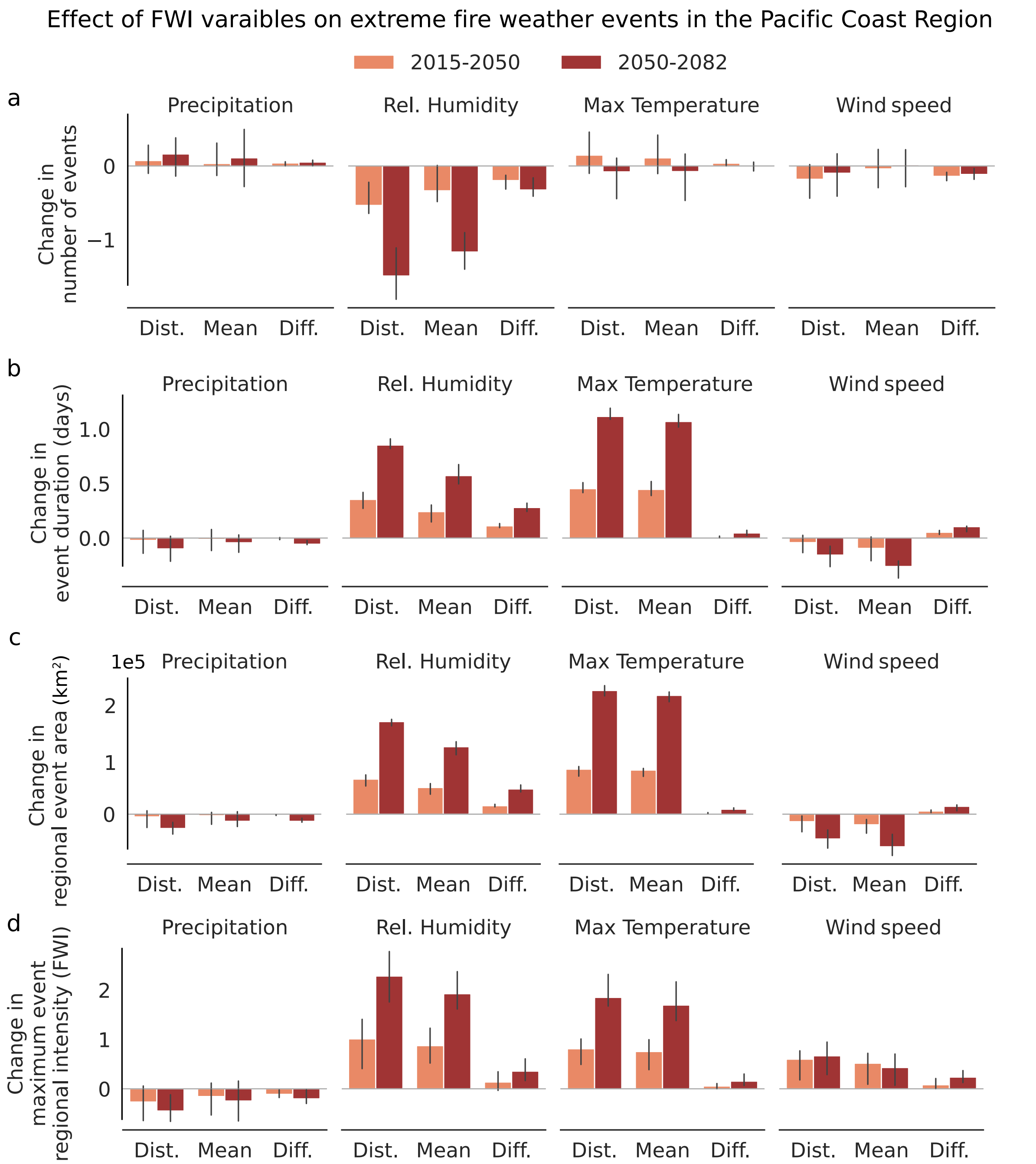


Fig. 10. The difference (from the historic period, 1980-2014) in the impact of changes in the full distribution (Dist.), mean, and variability (Diff.) of precipitation, relative humidity, maximum temperature and wind speed on (a) events per year, (b) events days per year, (c) regional event area, and (d) maximum regional event intensity FWI using the fixed threshold for the early (2015-2050, coral) and late future periods (2050-2082, red) for the Pacific Coast region. The mean across all events for each ensemble member is first calculated, and we show the median across all ensemble members. The error bar represents 20% of the ensemble spread from the median.

Compared to changes in mean maximum temperature, changes in mean relative humidity cause slightly smaller increases in the duration and area of extreme fire weather events in the future periods over the Pacific Coast region (Figures 9 s and F and 10 b and c). While changes in mean relative humidity do lead to increases in event frequency and intensity in eastern Oregon and Washington, they also lead to decreases in the coastal areas and in much of California (up to -0.8 events/year and -2 FWI units in intensity; Figure 9 f and S). Unlike for maximum temperature, we find that the changes in variability (obtained as the difference between the changes in distribution and mean) of relative humidity also lead to substantial and significant changes in event characteristics in much of the Pacific Coast, and tend to amplify the total impact of relative humidity changes on extreme fire weather events (Figures 9 g, t, G, T and 10). This is especially evident for event duration and area, where changes in the mean and variability of relative humidity lead to increases of 0.5 and 0.2 event days/year and 100,000 and 50,000 $km^2$ in average event area, respectively, in the late future period (Figure 10 b and c). The change in the mean of wind speed generally drives decreases in event duration and area over the region but causes increases in the frequency and intensity of events in southern California (Figure 9 l, y, L and Y). The impact of the changes in the variability of wind speed on event characteristics are relatively small in the region except for the intensity of events in northern California where there is an increase of about 4 FWI units (Figure 9 Z).

In the Four Corners regions, the impacts of changes in the mean and variability of the FWI variables are somewhat similar to those in the Pacific Coast region. Mean changes in maximum temperature and relative humidity lead to large increases in event days/year (up to 15 and 8 days/year, respectively) and area (up to 10,000,000 and 8,000,000 $km^2$, respectively) in the late future period (Figure 11 s, v, F, I). The impact of changes in the variability of maximum temperature is relatively small, however, changes in the variability of relative humidity lead to substantial and robust increases in event days/year and event area – approximately equal to the increases due to changes in the mean of relative humidity when looking across all events and ensemble members (Figure 12 b and c). Changes in the mean and variability of relative humidity also lead to spatially-varied impacts on the event intensity in the Four Corners region (Figure 11 S and T). For example, in the center of the region, there are small and not statistically significant changes in maximum intensity due to changes in the mean of relative humidity, but large and significant increases (approximately 6 FWI units, *p-value* $\leq 0.05$) due to changes in the variability. However, overall, changes in the mean of relative humidity lead to slight and non-robust increases in maximum event intensity, but changes in the variability lead to large and significant decreases (-0.5 FWI units in the late future period, *p-value* ≤ 0.05; Figure 12 d). Like the Pacific Coast, changes in the mean of wind speed also lead to overall decreases in the number of event days/year (-8 event days/year) and event area (-4,000,000 km$^2$), but are generally overwhelmed by the increases due to changes in other variables (compare Figure 11 Y and Z with N). However, in western Colorado, the large decreases in event intensity due to changes in windspeed mean (up to -10 FWI units) are also reflected in the changes due to all variables (up to -4 FWI units; Figure 11 N and Y).

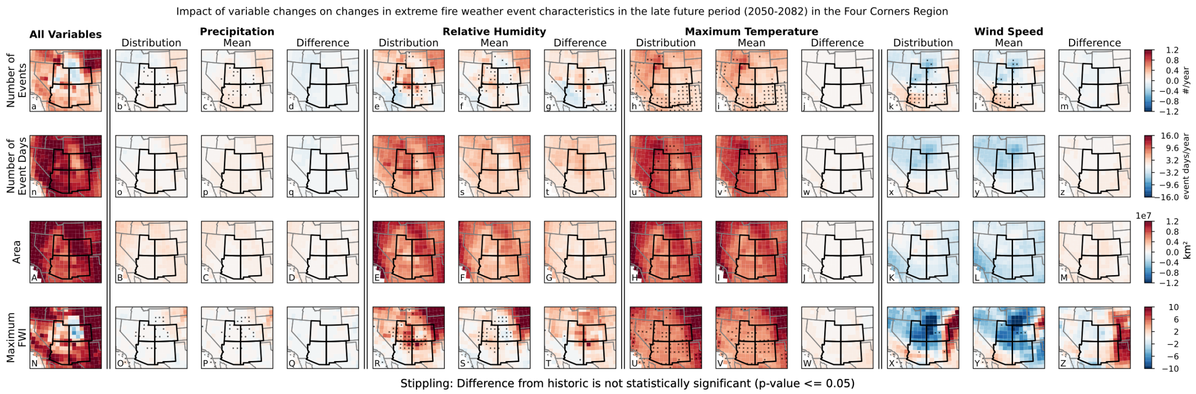


Fig. 11. The impact of changes in all variables (a, n, A, N), and the full distribution (b, e, h, k, o, r, u, x, B, E, H, K, O, R, U, X), means (c, f, i, l, p, s, v, y, C, F, I, L, P, S, V, Y) and variabilities (“difference”; d, g, j, m, q, t, w, z, D, G, J, M, Q, T, W, Z) of precipitation (b-d, o-q, B-D, O-Q), relative humidity (e-g, r-t, E-G, R-T), maximum temperature (h-j, u-w, H-J, U-W) and wind speed (k-m, x-z, K-M, X-Z) on changes (from the historic period, 1980-2014) in events per year (a-m), events days per year (n-z), event area (A-M), and maximum FWI (N-Z) using the fixed threshold in the late future period (2050-2082) for the Four Corners region. These composites are created by averaging event characteristics for all events for each ensemble member for each period at each grid point. Then, the grid point-specific values of the historic period are subtracted from each future period for each ensemble member, and the difference values are averaged over all ensemble members.

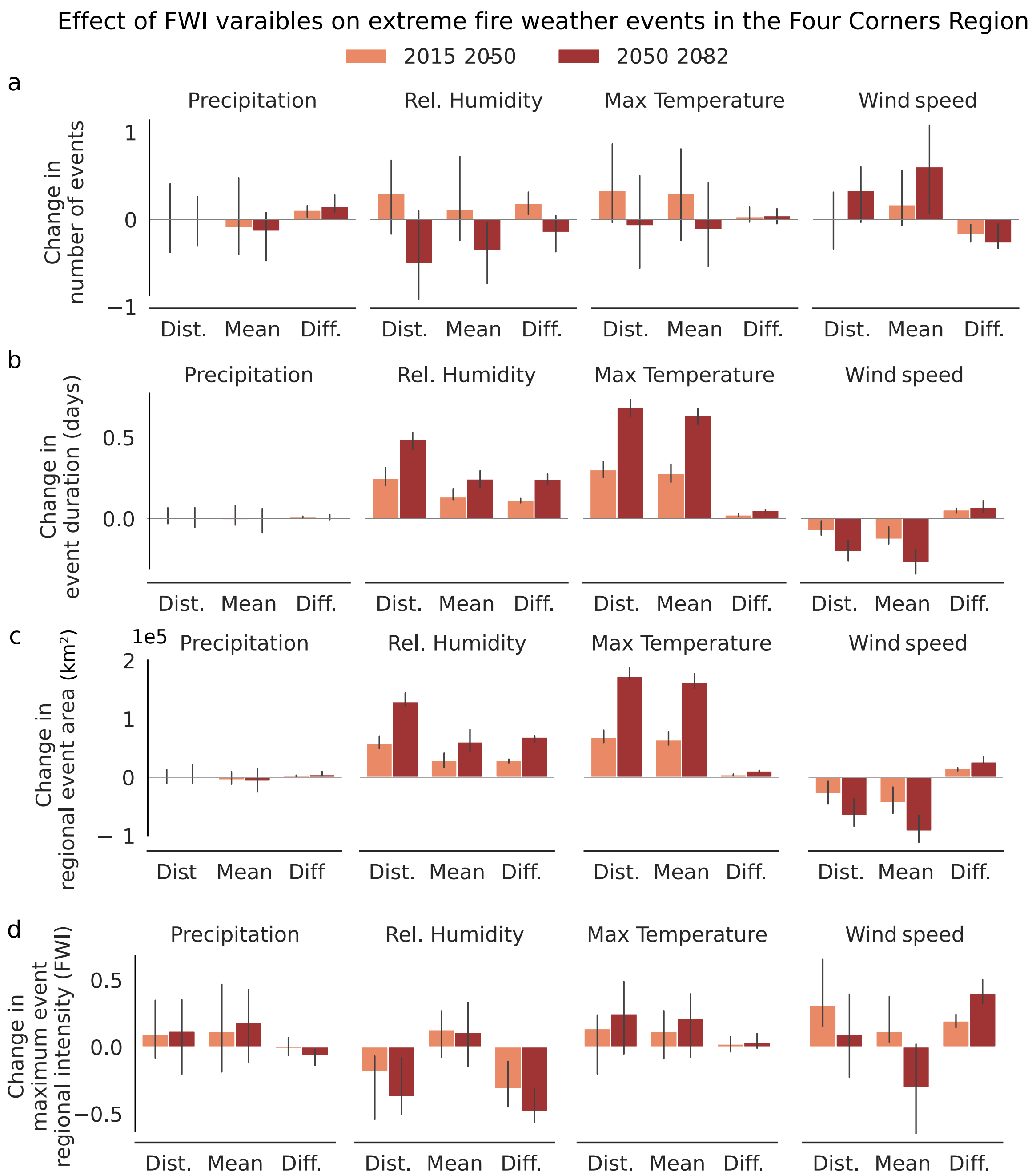


Fig. 12. The difference (from the historic period, 1980-2014) in the impact of changes in the full distribution (Dist.), mean, and variability (Diff.) of precipitation, relative humidity, maximum temperature and wind speed on (a) events per year, (b) events days per year, (c) regional event area, and (d) maximum regional event intensity FWI using the fixed threshold for the early (2015-2050, coral) and late future periods (2050-2082, red) for the Four Corners region. The mean across all events for each ensemble member is first calculated, and we show the median across all ensemble members. The error bar represents 20% of the ensemble spread from the median.

In both the Pacific Coast and Four Corners regions, changes in the mean of maximum temperature and in the mean and variability of relative humidity have the largest influences on extreme fire weather event frequency, duration, area and intensity. On the other hand, the impact of changes in wind speed are generally small, not significant, and varied, and changes in precipitation also plays a relatively small role in the changes of extreme fire weather event characteristics for both early and late future periods.

## 4. Discussion

Our study employs the CESM2 Large Ensemble to investigate projections of extreme fire weather event characteristics for current and emerging fire-prone regions, specifically, the Pacific Coast and Four Corners regions. Using a fixed threshold, we find that the frequency, duration, and area of extreme fire weather events are increasing, and events are extending well-beyond regional boundaries. By the end of the 21st century, events in the Pacific Region are expected to reach north towards Canada and east towards the Midwest, and events in the Four Corners regions are expected to reach northeast towards the Midwest and west and northwest towards Idaho, Nevada, and southern California. These increases in extreme fire weather event duration, area, and intensity are fueled by increasing maximum temperature means, decreasing relative humidity means, as well as changes in the variability of relative humidity that are not reflected in the mean changes. When using a moving threshold, event frequency, duration, and area are generally unchanging in the future periods, but some expansion of spatiotemporally connected events towards similar regions as the fixed thresholds is evident. Additionally, extreme fire weather events using a moving threshold are only slightly warmer than those in the historic period, but occur under much drier conditions, reflected in the underlying anomalously low precipitation and relative humidity.

We find that the choice of the baseline or threshold period used to investigate extreme fire weather events is highly important for making inferences about future events. In our case, we used two contrasting baselines: a fixed threshold that relies on the distribution of the FWI in the historical period only, and a moving threshold that accounts for an evolving FWI distribution. The relevance of a fixed *vs.* moving baseline for understanding the risk of extreme fire weather events in a particular region depends on the timescales at which communities and ecosystems adapt to changes in mean climate *vs.* climate variability. Similar considerations apply to other types of extremes, for example marine heat waves (Amaya et al., 2023; Deser et al. 2024). As far as we know, this is the first study to explicitly compare the impacts of projected changes in mean climate *vs.* climate variability on the characteristics of extreme fire weather events, and to quantify the underlying meteorological drivers of such changes.

By using a moving threshold, we can bring to light changes in event characteristics that may be due to changes in spatial or temporal variability of the FWI distribution that are not obvious when using a fixed threshold. We find some changes in extreme fire weather event characteristics when using a moving threshold, namely the underlying meteorological conditions that lead to extreme fire weather events, as well as the spatial connectivity of events in both the Pacific Coast and Four Corners regions. Moreover, we employed a relatively high FWI threshold to represent extreme fire weather days compared to previous studies (Abatzoglou et al. 2019; Touma et al. 2021). However, wildfire risk may also be present at lower FWI thresholds, especially in climatologically cold and wet regions. A lower threshold may show even greater changes in extreme fire weather event characteristics based on a moving baseline than the results reported here, given the greater opportunity for grid points and time steps to be spatiotemporally connected to each other.

To our knowledge, our study is the first to employ a quantile mapping method to isolate the changes in the mean and variability of the FWI variables to understand how they individually impact extreme fire weather events. We were able to robustly estimate the anthropogenically-forced changes in the mean and variability of the individual variables due to the availability of 100 CESM2 simulations that differ only by internal variability. While our findings show the large impact of increases in the mean of maximum temperatures and decreases in the mean of relative humidity that have been shown in previous studies (Abatzoglou et al. 2019; Jain et al. 2022; Touma et al. 2021), they also show that changes in the variability of relative humidity have a similarly large impact on extreme fire weather event frequency, duration, area, and intensity. In some areas of our study region, the impact of changes in the variability of relative humidity is equal to that of changes in the mean, doubling the total impact of relative humidity, which is a substantially larger estimate than that of previous studies (e.g., Zhuang et al., 2021). Our findings stress the need to consider changes in the variability as well as the mean of climate variables when understanding climate-change induced changes in different characteristics of extreme climate events, and therefore to employ large ensembles for assessing projections of extreme events.

By using a 35-year moving window that includes all daily values in our quantile-mapping method, we do not differentiate between different timescales of variability – daily to multi-annual timescales are considered together. Previous studies have shown that the El Nino Southern Oscillation (ENSO) and the Pacific Decadal Oscillation (PDO) influence the variability of wildfire occurrence over the pre-industrial and historical period in the western U.S., and that the Atlantic Meridional Oscillation (AMO) can also modulate ENSO's and PDO's influences (Kitzberger et al. 2007). Studies have also shown that ENSO's influence on wildfire danger in the western U.S. is expected to change in future years, as well as the influence on different wildfire-related variables (Fasullo et al., 2018).

We note that our study is one of many that shows that western U.S. wildfire risk is projected to increase over the next century, and that communities need to plan how to become resilient to these changes. By employing the moving threshold and understanding the role of variability and mean changes in our study, we also begin to shed light on how adaptation measures should be shaped. For instance, our study showed that extreme fire weather events are projected to spread over larger areas and become more spatially connected over the coming decades, highlighting the need to prepare for more widespread hazardous conditions. Our study also shows that by using a large ensemble, we capture the impact of forced changes in the variability of climate variables on extreme fire weather events. While the use of regionally downscaled (statistically and dynamically) climate projections is important for adaptation policy, they rarely include more than a few realizations and therefore could hide the impacts of the forced changes in climate variability (see Deser et al., 2020 for further reading). One way to overcome this issue is to statistically downscale global ESM Large Ensembles that are run at relatively coarse resolution or select a few "representative" ensemble members that could capture the forced changes in variability and use those to dynamically downscale climate projections (see, for example, Huang & Swain, 2022). While both pathways will lead to their own uncertainties, we stress the need to capture the impact of anthropogenic forcings on both the variability and mean of our climate system to quantify future risks of extreme fire weather events among other impacts.

*Acknowledgments.*

This material is based upon work supported by the NSF National Center for Atmospheric Research, which is a major facility sponsored by the U.S. National Science Foundation under Cooperative Agreement No. 1852977. We would like to acknowledge computing support from the Casper system (https://ncar.pub/casper) provided by the NSF National Center for Atmospheric Research (NCAR), sponsored by the National Science Foundation. We also acknowledge the CESM2 Large Ensemble Community Project and supercomputing resources provided by the IBS Center for Climate Physics in South Korea.

*Data Availability Statement.*

The CESM2-LE model output is available through https://www.cesm.ucar.edu/projects/community-projects/LENS2/data-sets.html. Analysis and visualization scripts will be made available through Zenodo upon publication.

REFERENCES

Abatzoglou, J. T., and A. P. Williams, 2016: Impact of anthropogenic climate change on wildfire across western US forests. *Proc. Natl. Acad. Sci. U.S.A.*, **113**, 11770–11775, https://doi.org/10.1073/pnas.1607171113.

——, ——, and R. Barbero, 2019: Global Emergence of Anthropogenic Climate Change in Fire Weather Indices. *Geophys. Res. Lett.*, **46**, 326–336, https://doi.org/10.1029/2018GL080959.

——, C. S. Juang, A. P. Williams, C. A. Kolden, and A. L. Westerling, 2021: Increasing Synchronous Fire Danger in Forests of the Western United States. *Geophysical Research Letters*, **48**, e2020GL091377, https://doi.org/10.1029/2020GL091377.

Amaya, D. J., and Coauthors, 2023: Marine heatwaves need clear definitions so coastal communities can adapt. *Nature*, **616**, 29–32, https://doi.org/10.1038/d41586-023-00924-2.

Andela, N., and Coauthors, 2017: A human-driven decline in global burned area. *Science*, **356**, 1356–1362, https://doi.org/10.1126/science.aal4108.

Balch, J. K., B. A. Bradley, J. T. Abatzoglou, R. C. Nagy, E. J. Fusco, and A. L. Mahood, 2017: Human-started wildfires expand the fire niche across the United States. *Proc. Natl. Acad. Sci. U.S.A.*, **114**, 2946–2951, https://doi.org/10.1073/pnas.1617394114.

Bui, H. X., Y.-X. Li, and D. Dommenget, 2024: Controlling factors of wildfires in Australia and their changes under global warming. *Environ. Res. Lett.*, **19**, 094030, https://doi.org/10.1088/1748-9326/ad69a9.

Burke, M., A. Driscoll, S. Heft-Neal, J. Xue, J. Burney, and M. Wara, 2021: The changing risk and burden of wildfire in the United States. *Proc. Natl. Acad. Sci. U.S.A.*, **118**, e2011048118, https://doi.org/10.1073/pnas.2011048118.

Collar, N. M., S. Saxe, B. A. Ebel, K. S. Boden, A. J. Rust, and T. S. Hogue, 2022: Linking fire-induced evapotranspiration shifts to streamflow magnitude and timing in the western United States. *Journal of Hydrology*, **612**, 128242, https://doi.org/10.1016/j.jhydrol.2022.128242.

Cook, B. I., and R. Seager, 2013: The response of the North American Monsoon to increased greenhouse gas forcing. *JGR Atmospheres*, **118**, 1690–1699, https://doi.org/10.1002/jgrd.50111.

DeRepentigny, P., and Coauthors, 2022: Enhanced simulated early 21st century Arctic sea ice loss due to CMIP6 biomass burning emissions. *Sci. Adv.*, **8**, eabo2405, https://doi.org/10.1126/sciadv.abo2405.

Deser, C., and Coauthors, 2020: Insights from Earth system model initial-condition large ensembles and future prospects. *Nat. Clim. Chang.*, **10**, 277–286, https://doi.org/10.1038/s41558-020-0731-2.

Dowdy, A., G. A. Mills, K. Finkele, and W. De Groot, 2009: *Australian fire weather as represented by the McArthur Forest Fire Danger Index and the Canadian Forest Fire Weather Index*. Centre for Australian Weather and Climate Research,.

Fasullo, J. T., 2020: Evaluating simulated climate patterns from the CMIP archives using satellite and reanalysis datasets using the Climate Model Assessment Tool (CMATv1). *Geosci. Model Dev.*, **13**, 3627–3642, https://doi.org/10.5194/gmd-13-3627-2020.

Fasullo, J. T., B. L. Otto-Bliesner, and S. Stevenson, 2018: ENSO's Changing Influence on Temperature, Precipitation, and Wildfire in a Warming Climate. *Geophys. Res. Lett.*, **45**, 9216–9225, https://doi.org/10.1029/2018GL079022.

Gallo, C., J. M. Eden, B. Dieppois, I. Drobyshev, P. Z. Fulé, J. San-Miguel-Ayanz, and M. Blackett, 2023: Evaluation of CMIP6 model performances in simulating fire weather spatiotemporal variability on global and regional scales. *Geosci. Model Dev.*, **16**, 3103–3122, https://doi.org/10.5194/gmd-16-3103-2023.

Goss, M., D. L. Swain, J. T. Abatzoglou, A. Sarhadi, C. A. Kolden, A. P. Williams, and N. S. Diffenbaugh, 2020: Climate change is increasing the likelihood of extreme autumn wildfire conditions across California. *Environ. Res. Lett.*, **15**, 094016, https://doi.org/10.1088/1748-9326/ab83a7.

Hoell, A., and Coauthors, 2022: Record Low North American Monsoon Rainfall in 2020 Reignites Drought over the American Southwest. *Bull. Amer. Meteor. Soc.*, **103**, S26–S32, https://doi.org/10.1175/BAMS-D-21-0129.1.

Huang, X., and D. L. Swain, 2022: Climate change is increasing the risk of a California megaflood. *Sci. Adv.*, **8**, eabq0995, https://doi.org/10.1126/sciadv.abq0995.

Jain, P., D. Castellanos-Acuna, S. C. P. Coogan, J. T. Abatzoglou, and M. D. Flannigan, 2022: Observed increases in extreme fire weather driven by atmospheric humidity and temperature. *Nat. Clim. Chang.*, **12**, 63–70, https://doi.org/10.1038/s41558-021-01224-1.

Jones, M. W., and Coauthors, 2022: Global and Regional Trends and Drivers of Fire Under Climate Change. *Reviews of Geophysics*, **60**, e2020RG000726, https://doi.org/10.1029/2020RG000726.

——, and Coauthors, 2024: State of Wildfires 2023–2024. *Earth Syst. Sci. Data*, **16**, 3601–3685, https://doi.org/10.5194/essd-16-3601-2024.

Juang, C. S., A. P. Williams, J. T. Abatzoglou, J. K. Balch, M. D. Hurteau, and M. A. Moritz, 2022: Rapid Growth of Large Forest Fires Drives the Exponential Response of Annual Forest-Fire Area to Aridity in the Western United States. *Geophysical Research Letters*, **49**, e2021GL097131, https://doi.org/10.1029/2021GL097131.

Kirchmeier-Young, M. C., F. W. Zwiers, N. P. Gillett, and A. J. Cannon, 2017: Attributing extreme fire risk in Western Canada to human emissions. *Climatic Change*, **144**, 365–379, https://doi.org/10.1007/s10584-017-2030-0.

——, and Coauthors, 2024: Human driven climate change increased the likelihood of the 2023 record area burned in Canada. *npj Clim Atmos Sci*, **7**, 316, https://doi.org/10.1038/s41612-024-00841-9.

Kitzberger, T., P. M. Brown, E. K. Heyerdahl, T. W. Swetnam, and T. T. Veblen, 2007: Contingent Pacific–Atlantic Ocean influence on multicentury wildfire synchrony over western North America. *Proc. Natl. Acad. Sci. U.S.A.*, **104**, 543–548, https://doi.org/10.1073/pnas.0606078104.

Lawrence, A. J., C. Matuch, J. J. Hancock, A. L. Rypel, and L. A. Eliassen, 2022: Potential Local Extirpation of an Imperiled Freshwater Mussel Population from Wildfire Runoff. *Western North American Naturalist*, **82**, https://doi.org/10.3398/064.082.0405.

Oakley, N. S., 2021: A Warming Climate Adds Complexity to Post-Fire Hydrologic Hazard Planning. *Earth's Future*, **9**, e2021EF002149, https://doi.org/10.1029/2021EF002149.

Raymond, C., and Coauthors, 2020: Understanding and managing connected extreme events. *Nat. Clim. Chang.*, **10**, 611–621, https://doi.org/10.1038/s41558-020-0790-4.

Rodgers, K. B., and Coauthors, 2021: Ubiquity of human-induced changes in climate variability. *Earth Syst. Dynam.*, **12**, 1393–1411, https://doi.org/10.5194/esd-12-1393-2021.

Sharma, A. R., P. Jain, J. T. Abatzoglou, and M. Flannigan, 2022: Persistent Positive Anomalies in Geopotential Heights Promote Wildfires in Western North America. *Journal of Climate*, **35**, 6469–6486, https://doi.org/10.1175/JCLI-D-21-0926.1.

Simpson, I. R., K. A. McKinnon, D. Kennedy, D. M. Lawrence, F. Lehner, and R. Seager, 2024: Observed humidity trends in dry regions contradict climate models. *Proc. Natl. Acad. Sci. U.S.A.*, **121**, e2302480120, https://doi.org/10.1073/pnas.2302480120.

Touma, D., S. Stevenson, F. Lehner, and S. Coats, 2021: Human-driven greenhouse gas and aerosol emissions cause distinct regional impacts on extreme fire weather. *Nat Commun*, **12**, 212, https://doi.org/10.1038/s41467-020-20570-w.

——, ——, D. L. Swain, D. Singh, D. A. Kalashnikov, and X. Huang, 2022: Climate change increases risk of extreme rainfall following wildfire in the western United States. *Sci. Adv.*, **8**, eabm0320, https://doi.org/10.1126/sciadv.abm0320.

——, J. W. Hurrell, M. R. Tye, and K. Dagon, 2023: The Impact of Stratospheric Aerosol Injection on Extreme Fire Weather Risk. *Earth's Future*, **11**, e2023EF003626, https://doi.org/10.1029/2023EF003626.

Virtanen, P., and Coauthors, 2020: SciPy 1.0: fundamental algorithms for scientific computing in Python. *Nat Methods*, **17**, 261–272, https://doi.org/10.1038/s41592-019-0686-2.

Wagner, C. E. V., 1987: *Development and structure of the Canadian Forest Fire Weather Index System*. Minister of Supply and Services Canada, 37 pp.

Williams, A. P., and Coauthors, 2022: Growing impact of wildfire on western US water supply. *Proc. Natl. Acad. Sci. U.S.A.*, **119**, e2114069119, https://doi.org/10.1073/pnas.2114069119.

Zhuang, Y., R. Fu, B. D. Santer, R. E. Dickinson, and A. Hall, 2021: Quantifying contributions of natural variability and anthropogenic forcings on increased fire weather risk over the western United States. *Proc. Natl. Acad. Sci. U.S.A.*, **118**, e2111875118, https://doi.org/10.1073/pnas.2111875118.

Zscheischler, J., and Coauthors, 2020: A typology of compound weather and climate events. *Nat Rev Earth Environ*, **1**, 333–347, https://doi.org/10.1038/s43017-020-0060-z.